Measurements of electron beam patterns and divergence using transverse optical probing with optical, XUV and Cu Kα X-ray imaging

K L Lancaster, J S Green*, C D Murphy*, R J Clarke, S J Hawkes, C Hernandez-Gomez, P A Norreys
Central Laser Facility, CCLRC Rutherford Appleton Laboratory, Chilton, Didcot, Oxon., OX11 0QX, UK

D S Hey, K U Akli****
*University of California, Davis, CA USA****

P Simpson, M Zepf
Departments of Pure and Applied Physics, Queens University, Belfast, UK

K Krushelnick
*The Blackett Laboratory, Imperial College London, Prince Consort Road, London, SW7 2BW, UK**

M H Key, R Snavely
*Lawrence Livermore National Laboratory, CA USA***

H Habara, R Kodama
Institute of Laser Engineering, Osaka University, Japan

M Nakatsutsumi, T Yabuuchi
Graduate School of Engineering, Osaka University, Japan

R R Freeman***
Ohio State University, Columbus, Ohio, USA

R Stephens
General Atomics, San Diego, CA, USA

C Stoeckl
Laboratory of Laser Energetics, University of Rochester, NY, USA

Main contact email address: *k.l.lancaster@rl.ac.uk*

Introduction

Knowledge of fast electron energy transport processes in over-dense laser plasma interactions is fundamental to the evaluation of the fast ignition concept. These mechanisms have been the subject of intensive investigation over the last few years. The first experiments using the Vulcan laser facility (published in 1998) indicated that the fast electron flow was collimated due to self-generated magnetic fields. This was inferred from shadowgrams obtained by a transverse optical probe taken 200 ps after the interaction. They showed that the expansion of the plasma from the rear surface of thick plastic targets was the same lateral size as the laser focal spot[1]. These measurements were made using 10 TW laser pulses. Jet-like structures inside transparent glass targets were also observed using the same technique by another team, the measurements being taken a few ps after the interaction pulse[2]. Gremillet *et al.*[3] later observed similar jets, but this was followed by a slower moving hemispherical ionization front. They concluded that there was only a small amount of energy in the jets imaged in the shadowgrams.

Optical measurements from the rear surface of thin foil targets (attributed to optical transition radiation and/or thermal emission) were made at the LULI[4] and GEKKO XII[5] 100 TW facilities. Divergent flow patterns were measured to be 34° and 25° respectively. Stephens *et al.*[6] later measured electron beam divergence of 40° using sandwich targets irradiated using the Vulcan and LULI laser systems at a similar intensity. The divergent flow was diagnosed using Cu K_α imaging of the rear surface with the Cu buried layer at different points in the target.

In this experiment, we undertook a comparison of the different measurement techniques - shadowgraphy, thermal radiation from the rear surface using optical and XUV imaging and Cu K_α imaging - on the same shots to see if there are any systematic differences between them. In general, we found that the observed fast electron flow patterns were divergent and the measurements were consistent with each other. However, the transverse optical probe showed interesting heating patterns that were not resolved in the other imaging techniques for very thin foil targets. The heating patterns were revealed 200 ps after the interaction in the shadowgrams, after considerable expansion of the plasma had occurred. The shadowgrams suggest that beam hollowing could be occurring in these thin foil target shots, and might be attributed to isochoric heating of the thin foils by the refluxing fast electrons. This hypothesis requires confirmation by computer simulations.

Experimental details

The experiments described in this report were conducted using the Vulcan Petawatt laser facility[7]. The Petawatt laser delivered up to 250 J of λ=1.05 μm light on to target contained in a pulse of duration 450 (±50) fs. The laser was focused on to target using an F/3 off axis parabolic mirror to a spot size of 7 μm diameter. Approximately 30% of the energy was contained within the central focal spot giving peak intensities of ~5×10^{20} Wcm^{-2}. The ASE of the laser was 5×10^{8} one nanosecond ahead of the interaction pulse. Closer to the main pulse, the contrast was between 10^{-6} and 10^{-8} and fluctuated on a shot by shot basis. The laser was incident onto target at an angle of 28°. The targets consisted of plain Cu, Al, and Al-Cu-Al sandwich targets to diagnose electron transport using K_α and XUV rear surface imaging. Transverse probing was used to image the global plasma expansion from the front and rear of thin Cu targets. Figure 1 shows a schematic of the experimental layout of the probe line and K_α imaging diagnostics.

An imaging system utilizing a spherically curved crystal was used to imaged Cu K_α (8.05 keV) radiation produced from Cu targets/layers. The Cu K_α emitted from the target was focused using a spherically curved crystal on to a Princeton Instruments 16 bit CCD camera. This produced an image of the emission region heated by the electron beam heating either a Cu buried layer or rear surface of a Cu target.

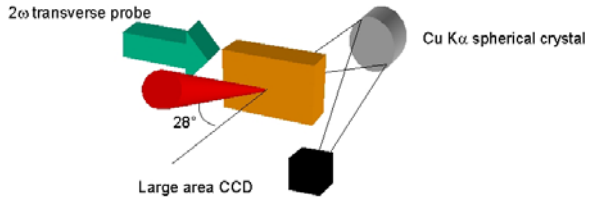

Figure 1. Experimental layout in TAP.

The expansion on the front and back surfaces of the target were diagnosed using a transverse probe. A small part of the main PW beam was leaked into the probe system (~8%). The 1.054 μm light is frequency doubled to 527 nm using a KDP crystal. The duration of the probe beam is the same duration as the main beam. An optical streak camera was used to synchronize the probe beam to the main beam. Images were taken at various times after the interaction up to 200 ps. At 200 ps, the expansion on the front and back surfaces could be observed for most target thicknesses. The shadowgraphy images were recorded using an eight-bit CCD camera connected to a personal computer via image acquisition software. The resolution of the probe system was found to be ~10-15 μm. Shadowgrams produced by this technique show dark regions where the density exceeds 10^{19} cm^{-3}, due to the large density gradients.

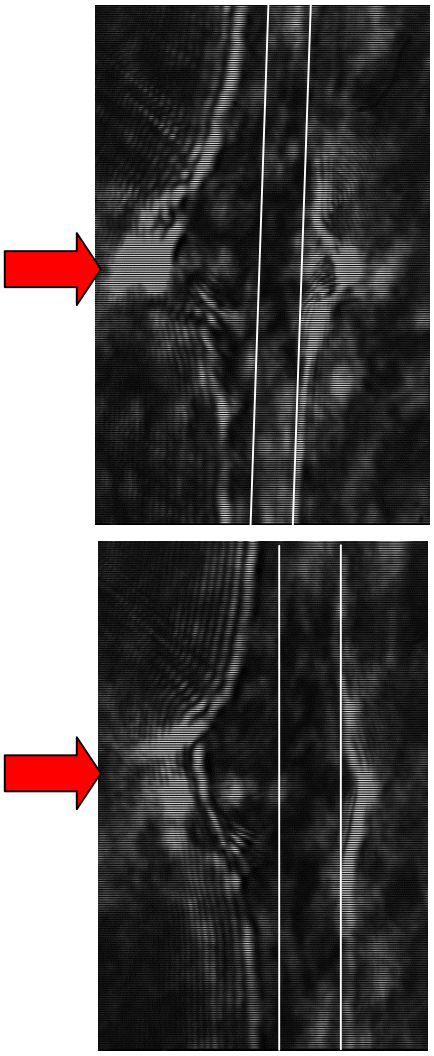

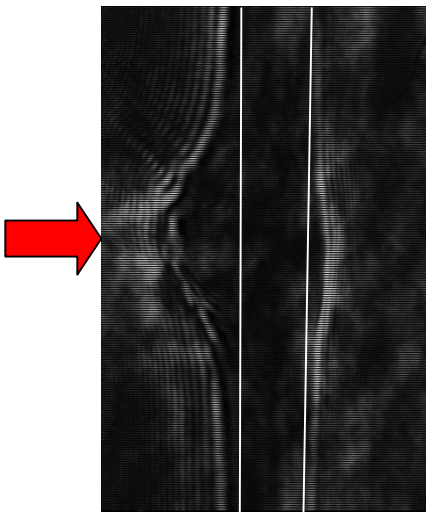

Figure 2. Shadowgrams of Cu targets of thickness a) 25 μm b) 50 μm c) 75 μm.

Results

Shadowgrams were obtained for a series of Cu targets of thicknesses 5 μm, 25 μm, 50 μm, and 75 μm. Figure 2 show shadowgrams taken at a time 200 ps after the interaction. Figures a, b, and c are Cu targets of thickness 25 μm, 50 μm, and 75 μm respectively. The expansion feature at the back surface shows the region that has been heated. These features were seen to increase in size as the target thickness was increased. This suggests that the electron beam heating the back surface is divergent. The divergence was estimated to be ~ 40^{o} from the change in size of the feature.

Cu K_{α} emission region sizes were also obtained. The spot sizes were obtained from measuring the FWHM of the Cu K_{α} image. The spot sizes were plotted against target thickness as shown in Figure 3. The divergence was calculated to be ~ 30^{o}.

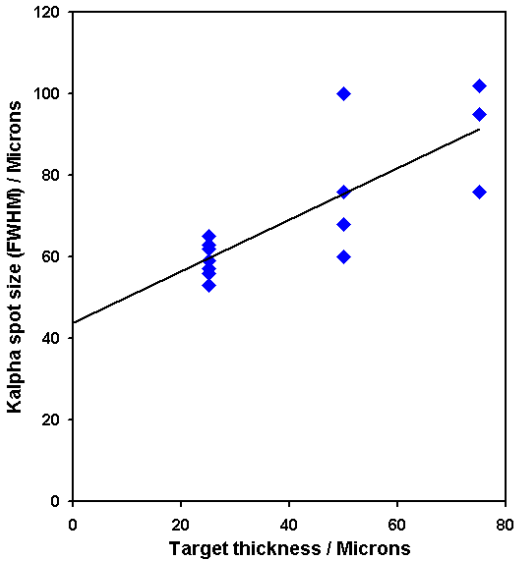

Figure 3. K_{α} spot size vs target thickness.

As described above, the pre-pulse varied on a shot-by-shot basis between 10^{-6} and 10^{-8}. Modeling of such contrast conditions was performed using the 2D hydrodynamic code POLLUX[8]. A Gaussian pulse of 3 ns long interacted with a 25 μm Cu target. The density scale length was recorded at a time of ~1.5 ns -2 ns, which correspond to the point in time when the main pulse would begin. The contrast at 10^{-6}:1 produced the scale length shown in Figure 4a. The critical surface is at ~5 μm at this contrast.

In Figure 2b, two regions of emission, attributed to self emission are visible. The first, less intense emission could be due to the pre-pulse. The second, brighter region could be self emission from the main pulse interacting with the preformed plasma. The two regions are separated by ~30 μm - 50 μm which suggests the contrast could have been worse. Figure 4b shows the density scale length produced from a contrast of 10^{-5}. This shows the critical surface is at ~22 μm. If the signal is really self emission it suggests the worst case contrast could be $>=10^{-5}$. The varying contrast has since been corrected at the OPCPA front end.

At a target thickness of 5 μm Cu, interesting features were visible at the front and back surfaces of the target. Figure 5 shows an image of a 5 μm Cu target taken at a time 200 ps after the interaction. On the back surface there is a triple humped feature which resembles an annular beam surrounding a central collimated region. The front surface expansion also has a triple humped feature. This pattern was observed only in the thinnest targets. These patterns were not visible in the XUV or K_α emission from the rear surface.

Discussion

It is interesting to note that similar expansion patterns from the back surface were observed in shadowgrams taken in previous experiments with the Vulcan 100 TW system for relatively thick plastic targets [9]. Those measurements showed that there is a transition between collimated and divergent flow regimes at 10 TW and 70 TW respectively in CH targets. The divergent flow had an annular shape consistent with the Davies' beam hollowing mechanism[10]. A triple humped distribution on the rear surface was observed on some shots that indicated that the collimated and divergent flow regimes could co-exist. This is possible because Ohmic heating of the target by the return current is time-dependent. According to the Davies' rigid beam model[10], if the target resistivity falls faster than linearly (which would occur if Spitzer resistivity is applicable to the return current) then the change in the electric field gradient will eventually lead to magnetic field reversal and a hollowing of the beam instead of pinching. This process will be dependent on the target material and Z. The minimum intensity for this to occur is ~10^{19} Wcm^{-2} for plastic targets. However, the increased heat capacity of metallic targets suggests that more deposited energy is needed in Cu targets for this process to occur. The observation of this transition may be consistent with the increase in laser energy to ~250 J and an intensity to ~5×10^{20} Wcm^{-2}.

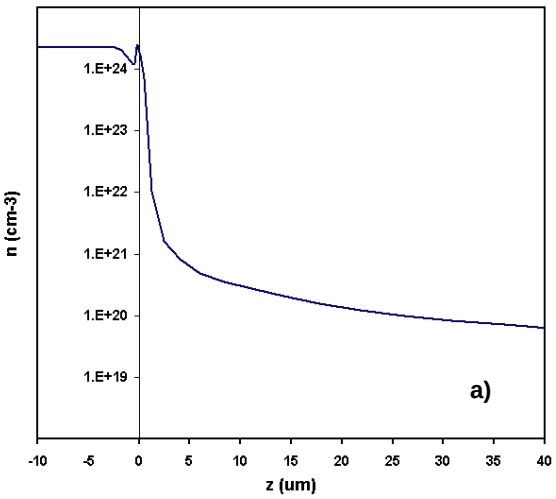

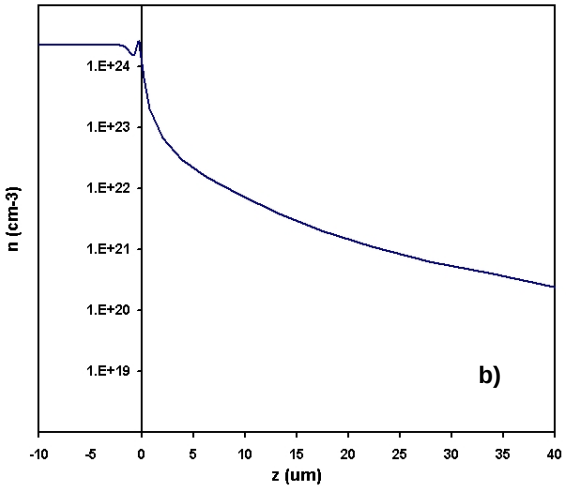

Figure 4. Density scale length generated using POLLUX with a contrast of a) $1:10^{-6}$ and b) $1:10^{-5}$.

Of course, the annular pattern could also be generated by fountain fields[11] at the back surface. The most energetic hot electrons escape the target and eventually the target potential prevents further loss of electrons. They are pulled back into the target at the rear surface. In the process, an azimuthal magnetic field around the electron beam is generated. An annular region around the central beam will be then heated. However this does not explain why the fountain field features disappear from the both the front and rear surfaces of the targets with thicker targets in Figures 2-4. Fountain fields would exist at the rear surface regardless of the target thickness.

On the other hand, an annular beam pattern could be generated once the temperature of the background plasma strongly enters the Spitzer resistivity regime. We speculate that this would require multiple reflections of the fast electrons from the rear surface, inducing large Ohmic heating of the background plasma by the return current. This heating effect would be reduced with increasing target thickness, since the number of reflections would be smaller within the laser pulse duration. Electrons that are reflected at the rear surface in an annular pattern can reach the front surface and heat the region either side of the initial interaction to create the triple humped feature there.

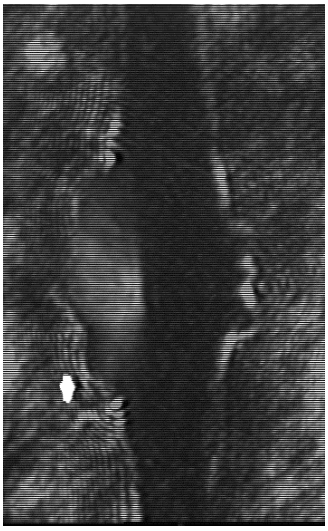

Figure 5. Shadowgram of 5 μm Cu target.

As noted above, this structure was not observed with the Cu K_α or the XUV images of the same shot. These measurements taken together suggest that only a fraction of the fast electrons are collimated and the type of the transport observed (collimated or diffusive) depends on the type of diagnostic employed. The spatially resolved Cu K_α emission will tend to "see" diffusive transport since this technique is sensitive to electrons with energies above the k-shell ionisation potential of Cu (i.e. > 8 keV), which is relatively small compared with fast electron beam energy. The XUV radiation from the heated region on the rear surface is optically thick and may not register small scale variations in temperature, particularly if some of the refluxing fast electrons travel along the rear surface and induce Ohmic heating there. Plasma formation on the back of the target will tend to see the collimated / annular transport patterns, while perhaps neglecting the diffusive element of the energy transport. Another misleading indicator from other experiments is the angular distribution of bremsstrahlung emission. Electrons collimated by a magnetic field will experience strong betatron oscillations leading to a broad radiation cone angle, so one cannot tell the difference between almost isotropic and collimated transport.

The fraction of collimated / annular transport depends of course on the target and fast electron parameters, which in turn depend on pre-pulse, pulse duration, intensity, wavelength, focussing, angle of incidence, target material and thickness. This complicated process indicates that many more experiments are needed in which each parameter is varied in a controlled manner.

Conclusion

We undertook a comparison of the different measurement techniques - shadowgraphy, thermal radiation from the rear surface using optical and XUV imaging and Cu K_α imaging - on the same shots to see if there are any systematic differences between them. In general, we found that the observed fast electron flow patterns were divergent and the measurements were consistent with each other. The expansion in Cu targets from shadowgraphy revealed a heated region that correlates with a divergent hot electron beam of ~ 40^o. This compared with ~30^o for the Cu K_α imaging. However, in 5 μm thick Cu foils, an annular heated region surrounding a collimated region was revealed. This may be explained by a transition between pinching and hollowing of some of the fast electron beam inside the target. The similar pattern at the front may be explained by refluxing of the annular beam from the rear surface. Clearly, computer simulations are necessary to distinguish these possibilities. These are now in progress.

References

1. M Tatarakis *et al.*, Phys. Rev. Lett. 81, 999 (1998)
2. M Borghesi *et al.*, Phys. Rev. Lett. 81, 112 (1998)
3. L Gremillet *et al.*, Phys. Rev. Lett. 83, 5015 (1999)
4. J J Santos *et al.*, Phys. Rev. Lett. 89, 025001 (2002)
5. R Kodama *et al.*, Nature (London) 412, (6849) 798 (2001)
6. R Stephens *et al.*, Phys. Rev. E 69, 066414 (2004)
7. C N Danson *et al.*, Nuc. Fusion 44, S239 (2004).
8. G J Pert, J Comput. Phys. 43, 111 (1981).
9. J Green *et al.*, CLF Annual Report 2004/2005, p 29
10. J R Davies, Phys. Rev. E 68, 056404 (2003)
11. A Pukhov, Phys. Rev. Lett. 86, 3562 (2002)